



HAL
open science

How Well Do EO-Based Food Security Warning Systems for Food Security Agree? Comparison of NDVI-Based Vegetation Anomaly Maps in West Africa

Agnes Begue, Simon Madec, Louise Lemettais, Louise Leroux, Roberto Interdonato, Inbal Becker-Reshef, Brian Barker, Christina Justice, Herve Kerdiles, Michele Meroni

► To cite this version:

Agnes Begue, Simon Madec, Louise Lemettais, Louise Leroux, Roberto Interdonato, et al.. How Well Do EO-Based Food Security Warning Systems for Food Security Agree? Comparison of NDVI-Based Vegetation Anomaly Maps in West Africa. *IEEE Journal of Selected Topics in Applied Earth Observations and Remote Sensing*, 2023, 16, pp.1641-1653. 10.1109/jstars.2023.3236259 . hal-04052591

HAL Id: hal-04052591

<https://hal.inrae.fr/hal-04052591>

Submitted on 30 Mar 2023










HAL is a multi-disciplinary open access archive for the deposit and dissemination of scientific research documents, whether they are published or not. The documents may come from teaching and research institutions in France or abroad, or from public or private research centers.

L'archive ouverte pluridisciplinaire **HAL**, est destinée au dépôt et à la diffusion de documents scientifiques de niveau recherche, publiés ou non, émanant des établissements d'enseignement et de recherche français ou étrangers, des laboratoires publics ou privés.



Distributed under a Creative Commons Attribution - NonCommercial - NoDerivatives 4.0 International License

How Well Do EO-Based Food Security Warning Systems for Food Security Agree? Comparison of NDVI-Based Vegetation Anomaly Maps in West Africa

Agnès Bégué , Simon Madec , Louise Lemettais, Louise Leroux , Roberto Interdonato , Inbal Becker-Reshef , Brian Barker , Christina Justice , Hervé Kerdilés , and Michele Meroni 

Abstract—The GEOGLAM crop monitor for early warning is based on the integration of the crop conditions assessments produced by regional systems. Discrepancies between these assessments can occur and are generally attributed to the interpretation of the vegetation and climate data. The premise of this article is that other sources of discrepancy related to the data themselves must also be considered. We conducted a comparative experiment of the growth vegetation anomalies routinely produced by four operational crop monitoring systems in West Africa [FEWSNET, GIEWS, ASAP, VAM] for the 2010–2020 period. We collected a set of normalized differences vegetation index-based indicators (% mean, % median, and Z-score) and proposed original methods to analyze and compare the spatio-temporal variations of these indices using Hovmöller representation, statistics, and spatial analysis. To facilitate systems comparison, a classification scheme based on the percentile rank values of anomaly indicators was applied to produce 3-class alarm maps (negative, absence, and positive anomalies). Results show that, on an annual basis, the per-pixel similarity is relatively low between the four systems [24.5%–34.1%], and that VAM and ASAP are the most similar (70%). The reasons of the products discrepancies come mainly from different preprocessing methods, especially the choice of the reference period used to calculate the anomaly. The negative alarm agreement classes show no eco-climatic zoning influence, but negative alarms hot-spots were locally observed. The negative alarm agreement maps can be a useful tool for early warning as they synthesize the information provided by the different systems, with a confidence level.

Manuscript received 27 August 2022; revised 8 November 2022 and 5 January 2023; accepted 8 January 2023. Date of publication 11 January 2023; date of current version 6 February 2023. This work was supported by the TOSCA-FRESA Project funded by the CNES (the French spatial agency). (*Corresponding author: Agnès Bégué.*)

Agnès Bégué, Simon Madec, Louise Lemettais, and Roberto Interdonato are with the UMR TETIS, University Montpellier, CIRAD, 34090 Montpellier, France (e-mail: agnes.begue@cirad.fr; simon.madec@cirad.fr; louiselemettais@gmail.com; roberto.interdonato@cirad.fr).

Louise Leroux is with the AIDA research unit, University Montpellier, CIRAD, 34090 Montpellier, France, and also with the International Institute of Tropical Agriculture, 00100 Nairobi, Kenya (e-mail: louise.leroux@cirad.fr).

Inbal Becker-Reshef is with the University of Maryland, College Park, MD 20742 USA, and also with Icube, University of Strasbourg, 67100 Strasbourg, France (e-mail: ireshef@umd.edu).

Brian Barker and Christina Justice are with the University of Maryland, College Park, MD 20742 USA (e-mail: bbarker@geoglam.org; justicec@umd.edu).

Hervé Kerdilés and Michele Meroni are with the European Commission Joint Research Centre, 21027 Ispra, Italy (e-mail: Herve.KERDILES@ec.europa.eu; Michele.meroni@ext.ec.europa.eu).

Digital Object Identifier 10.1109/JSTARS.2023.3236259

Index Terms—Agreement map, crop monitoring, early warning, Earth observation, food security, normalized differences vegetation index (NDVI) anomaly.

I. INTRODUCTION

WITH 15% of the total population affected by under-nourishment, food insecurity issues remain prevalent in West Africa [1]. High population growth, household food, and livelihoods-based primarily on low agricultural production due to low use of external inputs and rainfed conditions, and high rainfall variability are among the principal drivers of food insecurity. In addition to these factors, the security and health risks experienced by the region, have been exacerbated in recent times by the COVID-19 pandemic [2], making the agricultural production systems particularly fragile and fluctuating. Thus, the conjunctural aspects of agricultural production are combined with the structural aspects of the inherent vulnerability of the populations. Since the major droughts of the early 1970s, several global early warning systems (EWSs) for food security have been developed in the region to enable decision-makers to anticipate crises and to assist in planning emergency measures by targeting populations and/or areas at risk [3]. Since 2016, the Group on Earth observations, global agricultural monitoring [4] has published monthly GEOGLAM crop monitor for early warning¹ (CM4EW) bulletins that reflect an expert consensus among the main EWSs on crop growing status and conditions for the main crops in countries considered most at risk of food insecurity. To reach a consensus, the international organizations in charge of the various EWSs meet monthly to share their analyzes of crop conditions based primarily on EO data, agro-meteorological model outputs in addition to national reports field data and their own expertise, and discuss assessment discrepancies to ultimately reach a final conclusion on crop conditions [5]. The final consensus assessment is based on the CM4EW classification system comparing current crop conditions to the 5-year average. Classifications include exceptional, favorable, watch, poor, and failure. While there is often agreement in crop conditions assessments between organizations, discrepancies between

¹[Online]. Available: <https://cropmonitor.org/>

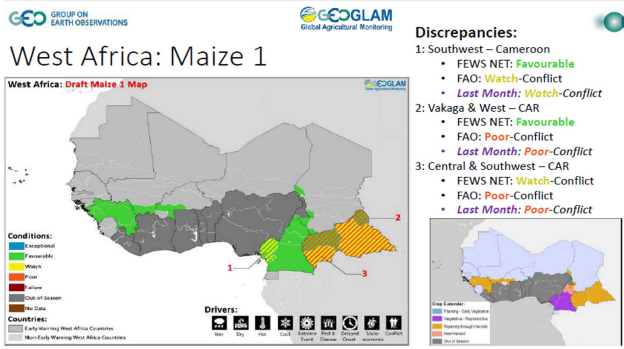


Fig. 1. Example of discrepancy map on the maize crop conditions in West Africa, as reported by two EWSs (FEWS NET and GIEWS); Source: Courtesy of GEOGLAM Crop Monitor.

organizations can occur when there is conflicting information from differing sources [5] (see Fig. 1); in areas where little reliable information is available from the field, priority is given to information that comes from converging remote sensing-based sources.

In these EWSs, satellite information is mainly used to derive vegetation index anomalies from low spatial resolution image time series to serve as proxies of crop health and status. The normalized differences vegetation index (NDVI) is the primary vegetation index for monitoring crop conditions. To this end, the NDVI value of the current compositing period (8-day or 10-day generally) is compared to the average NDVI value of the same period calculated over the previous years, or to what is assumed to be a normal situation, to provide an NDVI anomaly that can be used to track crop growing conditions throughout the season. These NDVI anomalies are used to draw conclusions on the vegetation status and potential impacts on agricultural yields and production.

In their review of the current operational global and regional agricultural monitoring systems, Fritz et al. [6] identified different gaps in data and methods. Because knowing which product to use in an environment where an increasing number of products are available remains a challenge, they recommend better understanding of the differences between different input datasets (precipitation and vegetation indices), in particular where these datasets have discrepancies, and to develop tools for automated comparison. The study presented in this article is in line with this recommendation and proposes, as a preliminary analysis, a comparative experiment of the growth vegetation anomalies produced by the crop monitors of the main EWSs in West Africa for the 2010–2020 period. To this end:

- 1) we collect a set of NDVI-based vegetation growth anomaly indicators (one per EWS) and develop a spatio-temporal approach to compare the extreme values;
- 2) we analyze and compare the spatio-temporal variations of these indices through space (with and without a cropland mask) and time (with and without a crop calendar masks), using statistics and spatial analysis tools.

The rest of this article is organized as follows. In the following section, we present the background of our study through a short review of the crop monitoring systems in West Africa. In Section III, we present the study area, the datasets used, and the

outlines of the methodology adopted. In Section IV, we present the statistical comparison between the systems and the systems agreement maps, which are then discussed in Section V. Finally, Section VI concludes this article.

II. SHORT REVIEW OF THE CROP CONDITIONS MONITORING IN THE EWSs IN WEST AFRICA

A. Agricultural Monitoring Systems in West Africa

In a recent study, Nakalembe et al. [7] reviewed the application-ready satellite-based agricultural monitoring systems covering West Africa. Four of these systems are partners of the GEOGLAM CM4EW [5], and are included in this study. The famine early warning systems network (FEWS NET) developed by USAID, the global information and early warning systems (GIEWS) of FAO, the Seasonal Monitor of the World Food Program (VAM), and the European anomaly hot spots of agricultural production (ASAP) system of the joint research center (JRC). However, because of their importance for West Africa, it is worth mentioning three other crop monitoring systems in the region: global agricultural monitoring (GLAM) of NASA, the University of Maryland, and the USDA Foreign Agriculture Service [8], the AGRHYMET system [9] of the permanent interstate committee for drought control in the Sahel (CILSS) that relies mainly on precipitation data and agrometeorological modeling, and CROPWATCH [10] of the RADI (Chinese Institute of Remote Sensing and Digital Earth) that reports crop (maize, rice, wheat, and soybean) conditions for Nigeria. These systems are not included in the study because, they either provide incomplete regional coverage, or the remote sensing data they use are shared with the previously mentioned systems.

B. Crop Conditions/Anomaly Indicators

The EWSs crop monitors use different data sources, but they all use optical data (NDVI-based) that provide information on crop development and vigor. The NDVI time series are used to calculate vegetation growth anomaly indicators that are then classified to produce vegetation anomaly maps that are published in regular bulletins and geoportals. These vegetation anomalies, in conjunction with other data sources (meteorological data, crop model simulations, field information, national/regional information) are used to provide a basis for the convergence of evidence of agricultural conditions that comprise the consensus based assessments under the GEOGLAM CM4EW [5], [11]. In some systems, additional data such as conflicts, market prices, and implementation of policies are used together with the agricultural conditions to alert national and international decision-makers on developing food security concerns impending food crises. Table I summarizes the characteristics of the main vegetation growth anomaly products used in the crop monitors of the main EWS of West Africa. In this article, only one NDVI-based anomaly indicator per system is used for analysis and comparison.

III. MATERIAL AND METHODS

Fig. 2 shows the flowchart of the data processing and analysis. Our work starts with the collection of the datasets of NDVI

TABLE I
DETAILS OF THE EO-DERIVED VEGETATION ANOMALY PRODUCTS USED IN THE CROP MONITORS OF THE EWSs IN WEST AFRICA; ONLY THE NDVI-BASED ANOMALY INDICATORS IN BOLD ARE USED IN THIS STUDY

| | FEWS NET | VAM | ASAP | GIEWS |
|------------------------------|---|---|---|---|
| Satellite product | eMODIS Level-1B Collection 6 (MODIS Terra & Aqua) | MYD13C1-MOD13C1 v006 (MODIS Terra & Aqua) | MOD13A2-MYD13A2 V006 (MODIS Terra & Aqua) | NOAA-AVHRR & METOP (since 2007) |
| Pre-processing | Weighted least-squares linear regression smoothing [12] | Whittaker filter | Whittaker filter | Weighted least-squares linear regression smoothing [12] |
| NDVI-based anomaly indicator | % median: NDVI | % mean: NDVI | z-score: NDVI , NDVI^c , mean: mNDVI^b | % mean: NDVI , VCI^c , VHI^d |
| Anomaly classification | Continuous values until +/-20% | 9 classes (extreme classes: +/-25%) | 7 classes (extreme classes: +/-2) | 9 classes (extreme classes: +/-15%) |
| Spatial resolution | 250 m | 5.6 km | 1 km | 1 km (since 2007) |
| Frequency | 10 days | 8 days | 10 days | 10 days |
| Time reference | 2003–2017 | 2002–2013 | 10/2001 to 12/2020 (NDVI) 10/2002 to 12/2020 (NDVI ^c) | 1984–2014 |
| Cropland mask | MODIS - LC (MCD12Q1) | FAO GLC Share | JRC Hybrid mask [13] | No |
| Crop calendar | Yes | No | Yes (1 or 2 seasons) | No |
| Web application | Early Warning eXplorer (EWX) | Hunger Analytics Hub | ASAP Warning Explorer | ASIS Global indicators |
| Publication | [14] | [15], [16] | [17], [18] | [19], [20] |

^aCumulative value of NDVI since the Start-Of-Season.

^bMean NDVI difference with historical average over the growing season period experienced until the date requested.

^cThe Vegetation Condition Index (VCI) is expressed in % and gives an idea of where the observed value is situated between the extreme values (minimum and maximum) in the previous years.

^dThe Vegetation Health Index (VHI) is based on both the Land Temperature Surface (LST) and the NDVI.

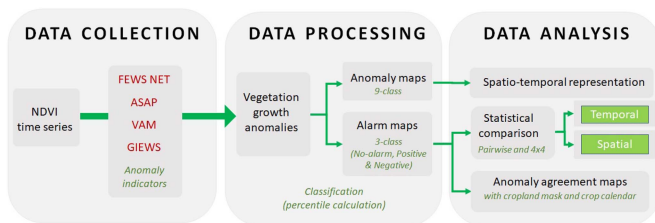


Fig. 2. Flowchart of the approach.

anomaly indicators of four EWSs, for the West Africa region over the 2010–2020 period. Then, to make values comparable in space and time, the anomaly values of the different products are harmonized over the whole area and period through percentile calculation to produce anomaly maps (nine classes) and alarm maps (three classes). These maps are then analyzed and compared at different spatial (national and regional) and temporal scales (annual and 11-year period), using statistics and spatial analysis tools.

A. Study Area

The study area is between 4.4°N and 18°N (the North Sahel limit) and 19°W–24.5°E, including 17 West African countries (see Fig. 3). West Africa's climate is controlled by the north-south movement of the Intertropical Convergence Zone (ITCZ). As a result, West Africa's precipitation regime is characterized by latitudinal belts of decreasing rainfall and wet season length. In the Guinean region, precipitation is abundant year-round with a bimodal pattern. As latitude increases, the amount of precipitation decreases, as well as the duration of the monomodal wet season. However, this latitudinal pattern is somewhat modified

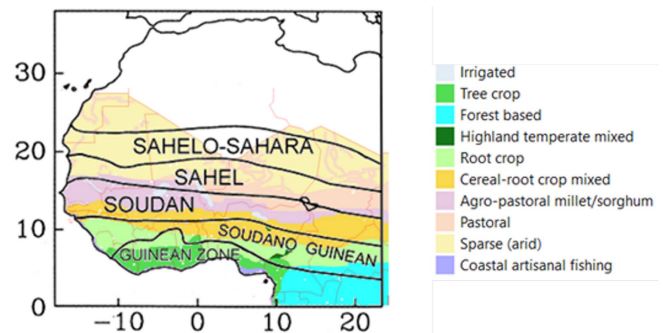


Fig. 3. Climate [23] and farming system [24] zone maps in West Africa.

by altitude, with higher mountain elevations (e.g., the Guinean Highlands and the Jos Plateau in central Nigeria), receiving more precipitation. The annual precipitation variability also becomes more significant with latitude, with a coefficient of variation around 0.3 in the Guinean region, to over 1.4 in the Sahel [21]. As throughout West Africa crops are mainly rainfed, the farming systems broadly follow the rainfall latitudinal gradient, with a system dominated by agro-pastoral millet and sorghum crops in the semiarid Sahel, by cereal-root crop mixed in the Soudanian part, by root crops in the Soudano-Guinean part, and by humid low-land tree crop in the Guinean part. According to Dixon [22], ten farming systems among the 16 possible over the continent are present in West Africa, illustrating the high diversity of the agro-environments in the study area.

Over the last decades, the study area experienced many environmental changes. In the Sahelo-Soudanian zones, since the drought period of the 1980s, an alternation of dry and wet years in the mid-1990s, followed by a rain resumption, is observed

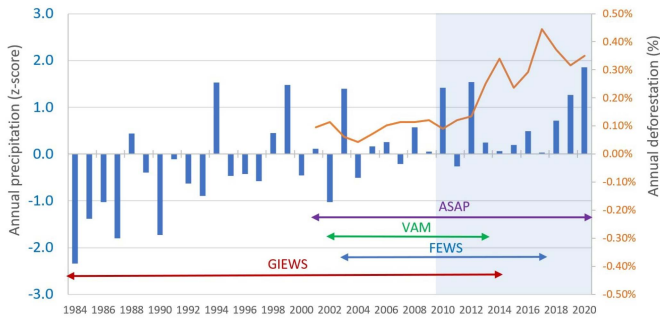


Fig. 4. Z-score of the annual precipitation (blue bars) calculated for the Soudano-Sahelian part (11.25°N and 13.75°N) of the study site (Source of data: GPCPMON v3.1.), and fraction of forest loss (orange line) calculated for the Guinean part (0° and 10°N) of the study site (Source of data: Hansen/UMD/Google/USGS/NASA). The colored horizontal lines indicate, for each system, the period of reference used to calculate the NDVI anomalies. The light blue area corresponds to the studied period (2010–2020).

(see Fig. 4); these variations seem to be linked to the surface temperature of the North Atlantic Ocean [25]. All over the study area, land-use changes are also observed [26], [27], in particular in the Guinean part characterized by an increasing deforestation rate since the 2010s (see Fig. 4).

B. Datasets Collection

1) *Anomaly Indicator Datasets*: Among the anomaly indicator datasets available for each system (see Table I), we chose only one anomaly indicator per system to simplify the analysis. Similarly, we restricted the study period to 2010–2020, which we felt was a good compromise between the amount of data to be processed and the inclusion of varied climatic conditions. The indicators were collected for the entire study area at their original spatial and temporal resolution (see Table I).

- 1) The anomaly indicators for the ASAP (NDVI z-score from the consolidated archive) and VAM (% of mean NDVI) systems were provided, respectively, by JRC and WFP.
- 2) FEWS NET anomaly indicators (% of median NDVI) were downloaded directly from the FEWS NET website.
- 3) GIEWS anomaly classes (9 classes built on % of mean NDVI) were downloaded from the GIEWS website. The anomaly values are not available, only the classes can be downloaded.

2) *Other Crop Datasets*: To focus the analysis on agricultural production, we constrained the data analysis in space and time, by using a cropland mask and a crop growing season mask, respectively. Among the readily accessible global, continental, and West African cropland masks [7], we used the Global Land Cover—SHARE [28] released in 2014 and composed of land cover datasets produced with satellite data acquired between 2008 and 2012. GLC-SHARE provides a set of 11 major thematic land cover classes among which the cropland cover class was used in this study. The spatial resolution of this dataset is 1 km, and the pixel value indicates the percentage of cropland within the area. We use a threshold of 10% to transform the dataset to a boolean cropland map (i.e., cropland = 1 if pixel > 10%, cropland = 0 else). The crop growing season was calculated from the phenological indices provided

by ASAP [17], which used an approach based on thresholds on the green-up and decay phases [29]. The start and end of a season was estimated through the historical average of the smoothed NDVI over the period 2002–2016 [18]. Two growing seasons were considered and maps were provided at a 1 km spatial resolution.

C. Dataset Processing

Data processing consists of the following:

- 1) anomaly data spatial aggregation at a common scale;
- 2) harmonization of the anomaly indicators;
- 3) classification of the harmonized anomalies.

Anomaly products are at different spatial resolutions (see Table I). To this end, all maps used in this study were resampled to a 1 km spatial resolution according to the ASAP product grid. To preserve the original anomaly values in the unaltered scene, the nearest neighbor resampling method was applied. Then, to ease the comparison and analysis of the different NDVI anomaly indicators used in the four crop monitoring systems (% mean, % median, and Z-score), a classification scheme was applied in two steps.

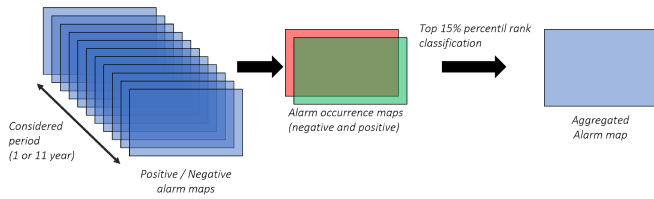
- 1) First, to harmonize the indicators, for each system the percentile rank values of anomaly indicators were computed from the entire dataset (all pixels of the study area, and all dates over the 2010–2020 period).
- 2) Then, 9-class (for qualitative comparison) and 3-class (for quantitative analysis) maps were produced.
 - a) The 9-class (referred hereafter as the Anomaly classes) correspond to seven 10-percentile classes between the 15th and 85th percentiles, plus two extreme classes (corresponding to the 15th percentile or less, and to the 85th percentile or more), and is close to GIEWS nomenclature.
 - b) The 3-class (referred hereafter as the Alarm classes) correspond to the two extreme percentile classes plus one median class (15th–85th percentiles); these three classes are labeled “negative alarms,” “positive alarms,” and “no alarm,” respectively. All the processing was performed using GDAL and Rasterio libraries with Python 3.9.

D. Dataset Comparison and Analysis

1) *Spatio-Temporal Representation of the Anomaly Classes*: Because of the marked latitudinal gradient of the vegetation in the West African region, a latitude-time Hovmöller diagram representation [30] was adopted to plot the 9 classes of NDVI anomalies. Furthermore, in order to be more consistent with agricultural production, we also produced spatially and temporally constrained Hovmöller diagrams using the cropland mask and the crop growing season mask.

2) *Statistical Comparison of the Alarm Maps*: For the spatial and temporal comparison of the anomaly products, a similarity metric is used. It corresponds to the proportion of pixels assigned to the same alarm class (i.e., for negative, positive, and absence of alarm) between systems. Similarity metrics were computed for different time steps (year, and 11-year period), and different system sets (pairwise, and 4×4). To synchronize the 8-day VAM product with the 10-day products (see Table I), we used the

Step 1 & 2 : Aggregation of alarm maps (for each four systems)



Step 3 : Generation of agreement maps between the four systems

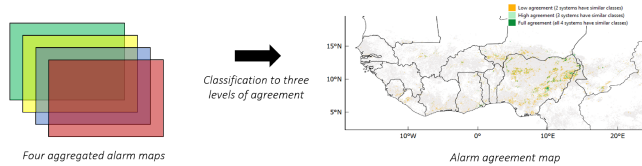


Fig. 5. Workflow of the production of the alarm agreement maps.

closest date (leading to a maximal shift of 2 days between VAM and the other products). In addition, Spearman’s rank correlation was calculated for pairwise systems comparison. Finally, the yearly percentage of the negative and positive alarms was computed, and the 2010–2020 trends of the different products were compared.

3) *Production of Alarm Agreement Maps*: Complementing the statistical comparison of the products, we produced agreement maps of alarm classes between the four systems at the regional and national scales. This was conducted in the following three steps.

- We computed annual and 2010–2020 aggregated alarm maps for each system, by calculating first the occurrences of the positive and negative alarm classes over each sq. km cropland and over the considered period, and then by applying a top 15% classification scheme on the number of occurrences.
- To reduce and filter out the errors related to georeferencing and rescaling the products from different spatial resolutions, a 3×3 majority filter was applied to the aggregated maps of the four systems.
- Finally, the filtered maps were merged to produce the agreement maps. These latter were prepared according to a classification scheme [6], [31] in which three levels of alarm class agreement are distinguished: Low agreement (pixels where two of the four systems are in agreement; it is possible that the other two pixels are identical to each other, no distinction was made); high agreement (pixels where three of the four systems are in agreement) and full agreement.

This process summarized in the Fig. 5 allows us to enhance spatial patterns of the level of agreement.

IV. RESULTS

A. General View

The spatial and seasonal variations of the harmonized crop growth anomalies are represented by the time-latitude Hovmöller diagrams in Fig. 6(a) (all data considered) and

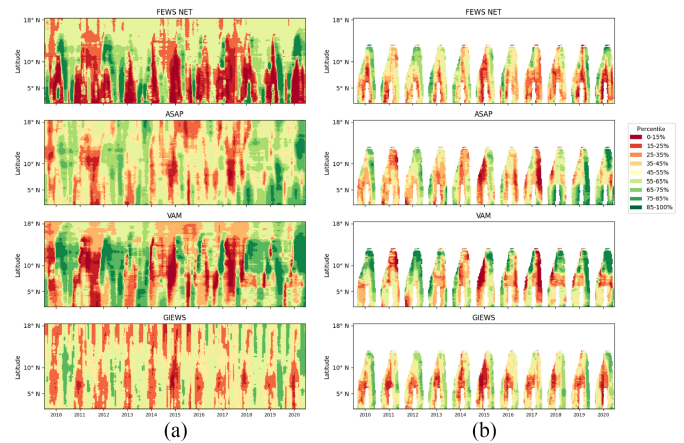


Fig. 6. Hovmöller (latitude-time) 2010–2020 plots for the study area (longitudes 19°W to 24.5°E), and (a) four crop monitors (1 km resolution) for all pixels and dates, and (b) for the cropland pixels and the growing season dates only. The colors represent the classes of harmonized vegetation growth anomalies.

Fig. 6(b) (after application of a cropland and a crop calendar masks) for the four crop monitors.

For the whole area and years [see Fig. 6(a)], we notice:

- large spatio-temporal discrepancies, with the extreme classes being strongly represented for FEWS and VAM, and less represented for ASAP and GIEWS;
- in terms of spatial patterns, we observe that the strong negative anomalies are concentrated in the Guinean and Soudano-Guinean regions ($<11^\circ\text{N}$) for FEWS NET, in the Soudano-Guinean and Soudanian regions (between 11°N and 14°N) for VAM. Positive anomalies are also particularly present in the Soudanian region for VAM;
- in terms of temporal patterns, GIEWS displays higher frequency of intermediate classes (25%–75% percentiles) than the other systems.

After masking the cropland and growing season masks [see Fig. 6(b)], we notice:

- the spatio-temporal discrepancies between the systems are less marked than when all the pixels and dates are considered. The global spatio-temporal variability of the NDVI anomalies is rather consistent between the systems (in particular the VAM and ASAP systems), even if the intermediate classes seem to be more represented in the GIEWS system compared to the others;
- as expected, we observe a monomodal annual cropping season in the Sahel and Soudanian regions, and a bimodal season in the Soudano-Guinean and Guinean regions. This Hovmöller representation permits to better analyze the crop conditions during the growing seasons; for instance, in the North of the study area, 2012 and 2020 present good conditions all along the season, while 2017 presents a good start and a bad end of the season. In the South of the study area, the two cropping seasons can display very different conditions within the same year—such as observed in 2012 for VAM, and 2018 for GIEWS—with bad conditions during the first season, and good conditions during the second.

TABLE II

ANNUAL SIMILARITY INDICES (EXPRESSED IN PERCENTAGE) OF THE 3-CLASS ALARM MAPS OF THE FOUR SYSTEMS; THE SIMILARITY INDICES ARE COMPUTED FOR THE WHOLE STUDY AREA AND ALL COMPOSITING DATES (“ALL PIXELS”), FOR CROPLAND AND ALL DATES (“CROPLAND PIXELS”), AND FOR CROPLAND AND CROP GROWING DATES (“CROPPED PIXELS”)

| Similarity | 2010 | 2011 | 2012 | 2013 | 2014 | 2015 | 2016 | 2017 | 2018 | 2019 | 2020 | Mean |
|-----------------|------|------|------|------|------|------|------|------|------|------|------|------|
| All pixels | 28.0 | 31.1 | 30.4 | 30.0 | 30.2 | 30.8 | 29.0 | 28.9 | 34.0 | 21.2 | 19.6 | 27.6 |
| Cropland pixels | 32.4 | 36.2 | 36.6 | 34.7 | 36.0 | 37.8 | 35.3 | 33.5 | 30.3 | 28.1 | 25.9 | 33.3 |
| Cropped pixels | 31.3 | 33.8 | 34.1 | 32.0 | 33.6 | 32.5 | 32.2 | 29.6 | 27.8 | 25.8 | 24.5 | 30.7 |

TABLE III

ANNUAL SIMILARITY INDICES (EXPRESSED IN PERCENTAGE) PER ALARM CLASS IN THE FOUR SYSTEMS; ONLY CROPLAND PIXELS AND THE CROP GROWING SEASON ARE CONSIDERED

| Similarity | 2010 | 2011 | 2012 | 2013 | 2014 | 2015 | 2016 | 2017 | 2018 | 2019 | 2020 | Mean |
|----------------|-------|-------|-------|-------|-------|-------|-------|-------|-------|-------|-------|-------|
| Negative alarm | 0.56 | 0.78 | 0.28 | 0.46 | 0.85 | 3.60 | 0.96 | 1.57 | 1.37 | 1.17 | 1.47 | 1.19 |
| Positive alarm | 1.91 | 0.67 | 2.04 | 1.84 | 2.10 | 1.25 | 1.53 | 1.41 | 2.52 | 5.02 | 3.18 | 2.13 |
| No Alarm | 28.87 | 32.33 | 31.82 | 29.69 | 30.67 | 27.68 | 29.70 | 26.58 | 23.92 | 19.60 | 19.87 | 27.34 |

TABLE IV

PAIRWISE ALARM CLASSES SIMILARITY BETWEEN THE FOUR SYSTEMS (EXPRESSED IN PERCENTAGE), CALCULATED FOR THE 2010–2020 PERIOD, FOR CROPLAND PIXELS, AND DURING THE CROP GROWING SEASON

| | FEWS NET | VAM | GIEWS | ASAP |
|----------|----------|-------|-------|------|
| FEWS NET | 1 | | | |
| VAM | 57.6 | 1 | | |
| GIEWS | 52.2 | 54.87 | 1 | |
| ASAP | 60.7 | 70.1 | 54.0 | 1 |

B. Statistical Comparison of the Alarm Maps

1) *Four Systems Comparison:* The similarity measure indicates the percentage of pixels with the same alarm class in the four systems (either positive, negative, or absence of alarm). Results in Table II show that, on an annual basis, the per-pixel similarity is relatively low, between 19.6% and 34%. This agreement increases when a cropland mask is used (5.7% average gain), and when a cropland and a crop calendar masks are used (3.1% average gain).

A deeper analysis of the four systems similarity (see Table III) indicates that the similarity percentage is mainly due to the “no alarm” class (between 19.60% and 32.33%), while only 0.28%–3.60% of the pixels are similar in terms of negative alarms, and 0.67%–5.02% are similar in terms of positive alarms. These low alarm similarity values must be brought back to the mean percentage of the positive and negative alarms proportions, which are each around 15% by construction.

In the following sections, only the cropland pixels and the growing season dates will be considered for analysis and comparison.

2) *Pairwise System Comparison:* The pairwise comparison conducted over the 2010–2020 period (see Table IV) indicates that the most similar systems in terms of alarm classes are the VAM and ASAP with around 70% similarity, followed by the ASAP-FEWS NET pair (around 61% similarity). The most divergent systems are FEWS NET and GIEWS (around 52% similarity). The conclusions are identical when using a Spearman rank correlation test (see Table V).

3) *Temporal Comparison:* Fig. 7 indicates the mean annual percentage of negative [see Fig. 7(a)] and positive [see Fig. 7(b)] alarms over the study area. As expected, the values are around

TABLE V

PAIRWISE SPEARMAN RANK CORRELATION BETWEEN THE FOUR SYSTEMS, CALCULATED FOR THE 2010–2020 PERIOD, FOR CROPLAND PIXELS, AND DURING THE CROP GROWING SEASON

| | FEWS NET | VAM | GIEWS | ASAP |
|----------|----------|------|-------|------|
| FEWS NET | 1 | | | |
| VAM | 0.08 | 1 | | |
| GIEWS | −0.01 | 0.11 | 1 | |
| ASAP | 0.11 | 0.25 | 0.06 | 1 |

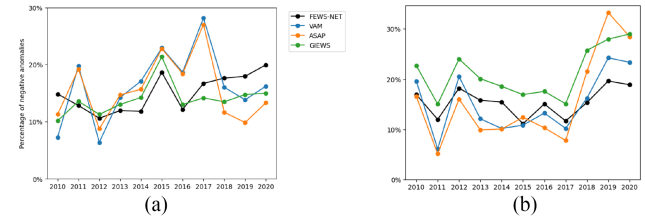


Fig. 7. Annual evolution of the percentage of (a) negative and (b) positive alarms calculated for the four EWSs, over West Africa and the 2010–2020 period; only cropland pixels and values during the crop growing season are considered. See text for more explanations.

15%—due to the methodology used to define the alarm classes—but the annual variability appears to be rather high, between 6.4% and 28.1% for the negative alarms, and between 5.1% and 33.3% for the positive alarms. Overall, VAM and ASAP show similar interannual patterns with close values of negative and positive alarm percentages and high interannual variability. FEWS NET and GIEWS, on the other hand, follow similar temporal patterns characterized by low interannual variations.

Considering the trends, the Pearson statistical test indicates a significant increase of the negative alarms for FEWS NET (p -value = 0.015), and a significant increase of the positive alarms for ASAP (p -value = 0.038). All other trends are not significant at a 95% confidence level. However, we observe for all systems an increase of the positive alarms for the last 3 years (2018, 2019, 2020) that was already visible on the Hovmöller diagrams (see Fig. 6).

C. Agreement Maps

1) *3-Alarm Classes:* Agreement maps between the alarm products derived from the four systems were produced for each year (see example of the year 2010 in Fig. 8(a); maps for the other years are provided in Appendix A), and for the whole 2010–2020 period [see Fig. 8(b)]. For the whole period, we observe about 28% of low agreements, and 72% of high and full agreements.

We then calculated the distribution of the anomaly classes agreement per country (see Fig. 9). Surprisingly, we observed no clear geographic pattern. High and full agreements are found in both some Sahelian (Senegal and Mali; >75%) and Guinean (Guinea and Gambia; >85%) countries, and, at the opposite, low and no agreement are found in other Sahelian (Mauritania; 39.7%) and Guinean (Sierra Leone; 46.7%) countries.

2) *Negative Alarm Classes:* We then focus on the negative alarm class, as it corresponds to areas that would require special attention for potential negative cropping outcomes and food security concerns. Fig. 10(a) shows the example of the 2010

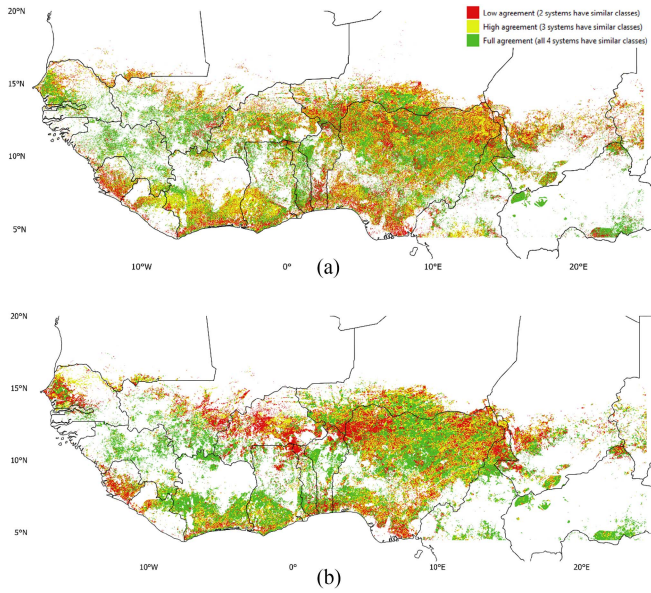


Fig. 8. Agreement map of the alarm classes (no alarm, negative and positive alarms) between the four systems, calculated for the cropland and the crop growing season only (see text for methodology) (a) for 2010 and (b) for the 2010–2020 period.

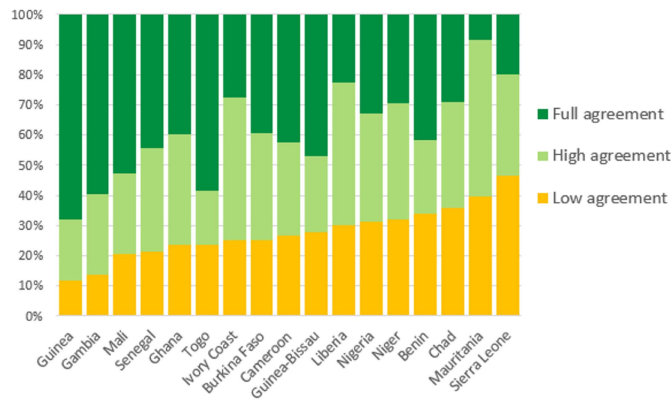


Fig. 9. Distribution of the agreement classes (low, high, and full agreement) between the four systems, calculated by West African country for the 2010–2020 period. The countries are ranked in (high + full) agreements descending order.

negative anomaly agreement map between the four systems (maps for the other years are provided in Appendix B). The negative class represents a small percentage of the area (by construction, around 15% of the area), but with clear spatial patterns. When integrated over the 2010–2020 period [see Fig. 10(b)], the spatial patterns of the negative alarms appear more clearly, with a score of 60% of high and full agreements between the systems (and 40% of low agreement).

When the 2010–2020 negative alarm agreement classes are calculated per country (see Fig. 11), we observe that Nigeria is the most consistent country, with 67.3% of full and high agreement, while Liberia and Sierra Leone are the least consistent countries with 100% and 96% of low agreement, respectively. It is also worth noticing that Guinea–Bissau shows no negative anomalies.

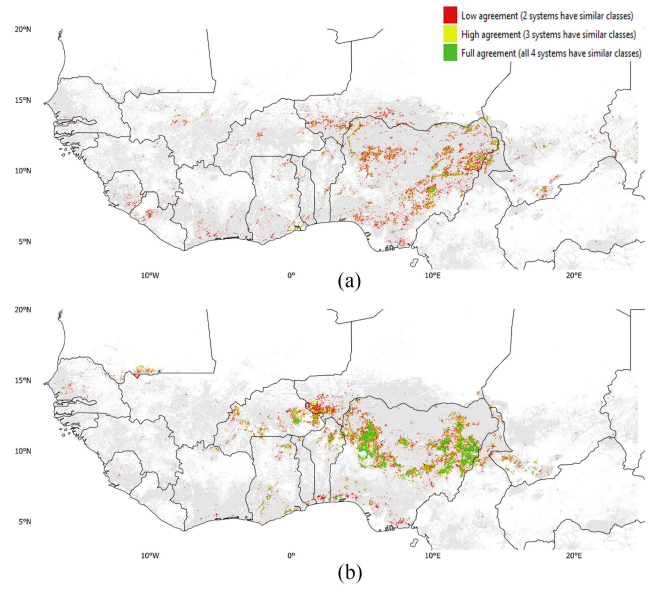


Fig. 10. Agreement map of the negative alarm class between the four systems, calculated for the cropland and the crop growing season only (see text for methodology), and (a) for 2010, and (b) 2010–2020 period. The grey area corresponds to the cropland.

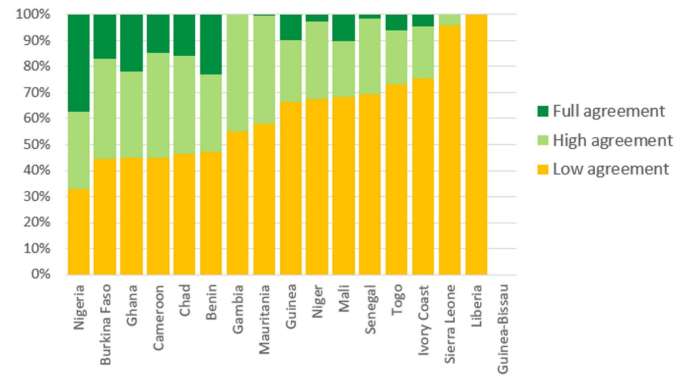


Fig. 11. Distribution of the negative alarm class agreement (low, high, and full agreement) between the four systems, calculated by West African country for the 2010–2020 period. The countries are ranked in (high + full) agreements descending order.

V. DISCUSSION

A. Comparison of the Anomaly Products

1) *Unexpected Discrepancies Between the Systems:* Because of the use of the same EO data (except for GIEWS), one would expect large similarities between the NDVI anomaly maps. The different results obtained show that it is not the case, both in space and time. The Hovmöller representation and the statistical analysis are the two tools used to characterize and quantify the discrepancies between systems.

Thanks to the north-south eco-climatic gradient in the region, the Hovmöller diagram has proven to be an interesting tool to illustrate the spatio-temporal variability of the NDVI anomalies in the region. It indicates a contrasted spatio-temporal distribution of the anomaly classes according to the systems, with extreme anomaly classes largely present for FEWS NET

(negative classes in the Guinean region) and VAM (both positive and negative classes in the Soudanian region). However, after filtering the pixels and dates that are outside the cropland and the growing season, respectively, the Hovmöller diagrams of the different systems seem more comparable. This effect is confirmed by the statistical comparison of the 3-alarm classes that show a similarity increase between the four products (from 27% to 30% on annual average).

The statistical comparison of pairwise systems also confirms the interpretation of the Hovmöller diagrams, with about 70% of similarity between the alarm classes of ASAP and VAM (Spearman correlation of 0.25), and only 52% of similarity between the alarm classes of GIEWS and FEWS (Spearman correlation close to 0).

2) *Potential Sources of Discrepancies*: Despite the fact that NDVI time-series data forms the core of all systems, we showed that the NDVI anomalies' spatial and temporal patterns show strong discrepancies that need to be understood. The anomaly products processing chains of the different systems can give elements to explain the differences. First, the NDVI data were calculated from reflectance data acquired by different EO satellites, MODIS for three systems, and NOAA-AVHRR and METOP data for GIEWS. This could partly explain the low similarities and correlations obtained between the products of GIEWS and those of other systems. Second, the algorithms used to smooth the NDVI time series differ between the crop monitoring systems. ASAP and VAM use the same algorithm, which could explain why they are quite similar, while the other systems use different preprocessing methods (see [32] for details about the eMODIS products used in FEWS NET).

It is easy to understand the importance of such algorithms, as cloud cover is still an important issue in the region. This point is particularly important for the analysis conducted during the crop growing season (the use of a crop calendar mask decreases the EWSs similarity measure calculated for the cropland; Table II), and in the coastal area of the Guinean countries, where large discrepancies are observed.

Third, to compare the systems, the anomaly indicators were spatially aggregated at a common resolution, which can contribute to noise in the information. However, the proximity of the ASAP (1 km) and VAM (5 km) systems indicates that the native spatial resolution of the products is not a major source of discrepancy. Finally, the vegetation anomaly indicator could play an important part in the system discrepancies. It is not so much the formula used to calculate the indicator, but rather the period chosen for the reference. Thanks to the harmonization carried out, the formula of the indicator, although different (z-score for ASAP and percentage deviation to the mean for VAM), should not have an important weight, while, on the contrary, the reference period can have an important impact on the value of the anomaly.

The reference period varies between 12 years, for VAM, to 30 years, for GIEWS. Yet, considering the high demographic growth and the rainfall variations in West Africa, important land use and vegetation conditions changes have occurred over the last decades [26], [33], in particular an increase of vegetation cover in the Northern part of the area, due to increasing annual rainfall [34], [35], and a decrease of vegetation cover in the

Southern part, mainly due to the deforestation [27]. These land processes occur at different time periods and places, introducing variations in the NDVI reference used to calculate the anomalies, and consequently in the anomaly values.

B. Agreement Maps, a Decision Support Product?

In addition to the quantification of the similarity between products for the extreme anomaly classes, this study aimed to provide alarm maps at regional and country scales that are qualified by the agreement score (full, high, and low). We produced agreement maps for the 3 alarm classes confounded, and for only the negative alarm class that, a priori, is the most important class for food security and early warning. The maps were postprocessed with a 3×3 majority filter. This smoothing strategy allows for a more general overview of spatial trends and eases visual interpretation. This also filters out the noise due to the resampling of the products with varying resolutions and errors in georeferencing.

Regarding the alarm maps (3 classes), 28% of low agreement were observed in contrast to the 72% of high and full agreements for the whole considered period (2010–2020) and cropped pixels. As previously mentioned, these agreements are higher than the scores of the pixel-per-pixel similarity. This is explained by the classification scheme used to aggregate the 10-day period alarm maps. Indeed, classifying the pixels with the top 15% occurrence of negative and positive anomalies as, respectively, negative and positive alarm classes increases the similarity between the products for a given period. We observed on the maps that low agreements are mainly located in the coastal area of the Guinean countries (Sierra Leone, Ivory Coast, Ghana, Benin, Togo, and Nigeria). The high presence of clouds in this area may bring some differences in the vegetation alarm maps computed from the different products, with different temporal filtering.

For the negative alarm maps, the agreement between systems is less with about 40% of low agreement class, and 60% of cumulated high and full agreement class, for the whole period and area. This result was expected as the no-alarm class represents a large percentage of the total similarity between systems. The negative alarm agreement results show no eco-climatic zoning influence at the country level, but we observed a spatial pattern of negative alarms with hot-spots in the Tillabery (South West Niger), East and Center-East (Burkina Faso), and Alibori (North Benin) regions, and two large areas in Central and North-East Nigeria, for the 2010–2020 period. The annual and decadal negative alarm agreement maps can be a useful tool for early warning, by helping to prioritize the emergency measures. These maps synthesize the information provided by the different crop monitoring systems and provide information on the confidence level associated with the negative anomaly through the agreement class. However, we should keep in mind that negative alarms are not always synonyms of a decrease in agricultural production. Land cover changes inside a pixel, such as deforestation in the southern part of the study area, can result in a decrease of NDVI without necessarily being linked to a decline of crops conditions in the area. At the opposite, pixels classified as positive alarms can correspond to a decrease of

agricultural production in particular in the Sahel region where the abandonment of cultivated land results in an increase of NDVI because natural vegetation has higher NDVI than crops in this region [36]. So, it is important to keep in mind that land cover or land use changes can induce NDVI anomalies that are not linked to crop conditions anomalies. Data on land cover dynamics, such as the forest cover change [37] or the cropland change [38] maps, should, thus, be included in the assessment of crop conditions.

C. Study Limitations

Despite important methodological and thematic contributions, we are aware that the study has certain limitations related to both the datasets and the comparison method used.

In terms of datasets, the first limitation is that only one type of NDVI-based anomaly products was considered, while other crop conditions indicators exist (see Table I). NDVI shortcomings are well known (atmospheric noise, saturation for high levels of biomass, etc.), but NDVI remains a robust index [39], well correlated to the active vegetation amount, and available on all (optical) satellite platforms from the beginning of EO. The second limitation is that the NDVI-based anomaly products used in the study are different in nature (anomaly classes for GIEWS, and anomaly values for the other systems).

In terms of data processing, the spatial and temporal re-sampling of the initial products could have introduced some bias. Likewise, the alarm classes are defined using an arbitrary threshold of 15% of the extreme percentiles, and the results could have been different with another threshold value. Another method limitation is the use of a unique cropland map for the whole period of analysis (11 years); it is well known that for the last four decades, West Africa has experienced large land use changes fueled by high demographic growth, with an increase of cropland, replacing and fragmenting savannas, woodlands and forests [27]. In the same way, the use of a unique growing season calendar for the whole study period is problematic because West Africa is well known for the high variability of its rainfall pattern and therefore crop phenology; Furthermore, this calendar is derived from land surface phenology metrics, and even when considering only cropland pixels (that are in reality mixed cropland-natural vegetation pixels), it is improper to consider it as a crop calendar.

Finally, the main limitation of the study remains that we only compare, not order, the NDVI anomaly products. The product hierarchization was not part of the study, but should be a priority for the next studies. Research perspectives on this topic are presented in Section VI.

D. Future of EO-Based Crop Monitors

While NDVI anomalies are the focus of this article, the EWSs use other types of remote sensing variables to assess the crop and rangeland conditions, such as thermal infrared data to compute the temperature conditions index, brightness temperature to derive soil moisture or precipitation data to compute the water requirement satisfaction index (GWSI). Likewise, high spatial resolution satellite time series (Sentinel 1 and 2, and Landsat)

are already used in some EWSs to focus on particular areas. For example, ASAP² offers the possibility to access and analyze these high resolution data at the field level, but the full capacity offered by such data is not fully and systematically exploited. The arrival of new data in the field of Earth observation and the enormous progress in data processing pave the way for a new generation of EWS. At short-term, for national and regional early warning products based on vegetation anomalies, improvements are expected to come mainly from the methods, more than from new Earth observation mission, because the new EO systems are too recent to offer sufficiently long reference periods (5 years of data available so far for Sentinel-2 constellation, for example). Because of NDVI limitations (atmospheric noise, saturation for high levels of biomass, etc.), other spectral indices could be tested such as EVI that is thought to have a greater sensitivity to high density canopies, and a lower sensitivity to the atmosphere, but whose benefits compared to the NDVI are questioned in the literature (e.g., [40], [39]). Other spectral indices including short-wave infrared band (e.g., NDWI, NDMI), for estimating vegetation water content, or green band (e.g., GCVI, GNDVI) for estimating the vegetation nutrient concentration, could also be tested in West Africa where water and nutrients are limiting factors of crop productivity. Another short-term improvement of the crop monitors, could be the use of agro-ecological zones (e.g., GAEZ; [41]) to calculate and classify the anomalies percentiles. Zone-specific alarm class maps could be more meaningful to assess potential impacts on agricultural yields.

At mid-term, significant advances are expected from the following.

- a) The ancillary products, such as more accurate cropland and crop group masks using Sentinel data, and more accurate detection of the growing season (start and end of season)
- b) Data processing, in particular improved image time series preprocessing (NDVI smoothing or gap-filling), real-time processing, and cloud-computing.
- c) Improved data and products access (cf. new opportunities offered by initiatives such as the africa regional data cube/digital earth africa).
- d) Improved decision support products, more readable by decision makers (cf. GEOGLAM).

Coarse-resolution crop monitoring systems are essential for decision-makers, and we are not convinced that vegetation anomaly maps produced at a higher spatial resolution would be better for national or regional crop monitoring as, to cite [20], it is very difficult for a government to take actions at a granular level lower than the district or municipality, such as a farm or commune. The future for EO crop monitoring will certainly include data from the next generation of hyperspectral and thermal satellites with higher spatial resolution and revisit time. Finally, all these improvements will benefit from advancements in computer science that will help to combine heterogeneous data, such as EO data, crop model simulations, numeric media

²[Online]. Available: <https://mars.jrc.ec.europa.eu/asap/hresolution>

data, and crowd-sourced data in order to support regional and national EWSs.

VI. CONCLUSION

GEOGLAM, the GLAM system of systems, ensures the coordination and information sharing of the regional and national systems [42]. The coordination under the GEOGLAM CM4EW requires comparing and integrating crop conditions assessments produced by systems that integrate vegetation and climate anomalies, ground observations, and other information sources and synthesizing these efforts into a consensus-based assessment that represents the agreement of the EWSs involved. Discrepancies between these assessments can occur, for many reasons [5]. One source is certainly the interpretation of these data, which varies with the data source and the expert sensitivity. Our study reveals that, upstream of the crop conditions mapping, the different NDVI anomaly maps produced and used by the different systems are surely another source of discrepancy.

The main contributions of this study are methodological and thematic. In terms of method, to the best of authors' knowledge, it is the first study to compare the vegetation anomalies component of the CM4EW systems. We developed an original approach to visualize and compare the vegetation anomalies both in time and space. In terms of thematic, this study reviewed the crop monitoring systems implemented for West Africa, in particular the NDVI anomaly products used, and identified potential reasons that could lead to discrepancies in crop conditions assessments. These reasons are multiple, but seem to come mainly from different preprocessing methods used, especially the NDVI smoothing algorithms and the reference period used to calculate the anomaly. NDVI smoothing is particularly sensitive in the Guinean part of West Africa, where the satellite image time series are noisy due to a dense cloud cover, resulting in a high discrepancy between the systems. However, the issue of low confidence in the alarm class is somewhat mitigated by a lower food security risk in this region (the area is less prone to yield reduction caused by a lack of water) compared to the other regions of West Africa. We also showed that the choice of the reference period was particularly important in West Africa, where the environmental and land use changes are strong. We therefore recommend careful study of the reference period selected, and in regions where there have been large changes in land cover or climatic conditions, we recommend using a shorter reference period. Another important output of this study is the production of synthetic decadal and annual alarm agreement maps. These agreement maps can be a useful tool for early warning by helping to prioritize the emergency measures in hot-spot areas displaying negative alarms and a high level of reliability (expressed in number of concordant systems).

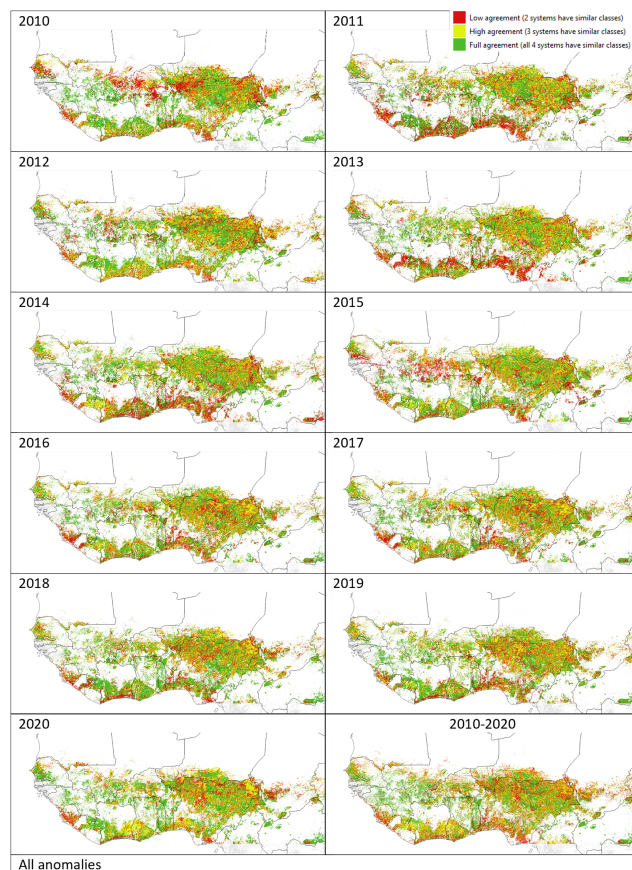
Like any study, this work has certain limitations, but they are not penalizing considering the objective of comparison of anomaly products in time and space. However, it is obvious that the next steps will be to better understand these differences and to hierarchize the systems for different applications or different geographic regions. For the first step, we can use the same

reference period for the long term statistics, resample row data at the same resolution, and compute different anomaly indicators from the same NDVI dataset. For the second step, we will need external data to evaluate the temporal and spatial consistency of the different systems, and thus, make recommendations. For the first step, we can use the same reference period for the long-term statistics, resample row data at the same resolution, and compute different anomaly indicators from the same NDVI dataset. For the second step, we will need external data to evaluate the temporal and spatial consistency of the different systems, and thus make recommendations. Ideally, these data would be crop yield statistics, provided they are collected following a sound methodology and not "harmonized" in the aggregation process. Alternatively, we could use the outputs of agrometeorological or crop models (such as SARRA-O model, for the West African region [43]), or the results of automatic language processing methods applied to media data such as online newspapers [44].

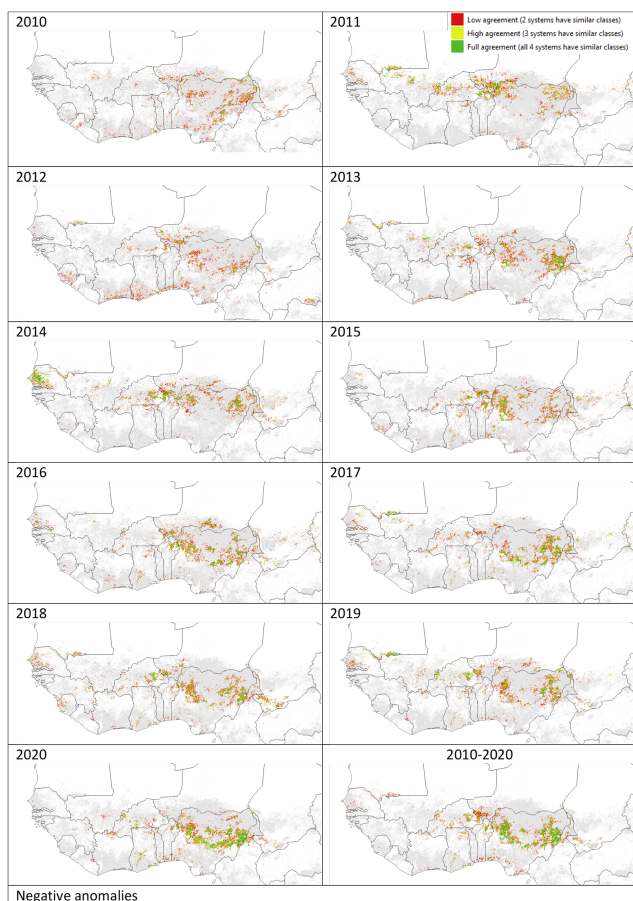
To conclude, this work is a contribution to the upstream process of the food security data processing chain. Recognizing the importance of reducing sources of uncertainty for monitoring food insecure areas, this work shines a light on important sources of discrepancies between systems that should be considered for effective agricultural lands monitoring.

APPENDIX A

ANNUAL AND 2010–2020 SYNTHETIC AGREEMENT MAPS FOR THE 3 ALARM CLASS (NO ALARM, POSITIVE, AND NEGATIVE)



APPENDIX B
ANNUAL AND 2010–2020 SYNTHETIC AGREEMENT MAPS FOR
THE NEGATIVE ALARM CLASS



ACKNOWLEDGMENT

The authors would like to thank R. Bonifaccio from WFP for kindly providing the NDVI anomalies data, and O. Rojas from FAO for sending information about ASIS.

REFERENCES

- [1] FAO, IFAD, UNICEF, WFP, and WHO, "The state of food security and nutrition in the world 2020," FAO, IFAD, UNICEF WFP, and WHO, 2020. [Online]. Available: <http://www.fao.org/documents/card/en/c/ca9692en>
- [2] FEWSNET, "Drivers of acute food insecurity in 2020," *Global Special Rep., USAID*, Jul. 2020, p. 4. [Online]. Available: https://fewsn.net/sites/default/files/documents/reports/Special_Report_Globa_Drivers%20of%20Acute%20Food%20Insecurity%20in%202020_07312020_0.pdf
- [3] L. Genesio et al., "Early warning systems for food security in west africa: Evolution, achievements and challenges," *Atmospheric Sci. Lett.*, vol. 12, pp. 142–148, 2011. [Online]. Available: <https://onlinelibrary.wiley.com/doi/10.1002/asl.332>
- [4] "Geoglam—EW crop monitor," 2021. [Online]. Available: <https://cropmonitor.org/index.php/eodatatools/cmet/>
- [5] I. Becker-Reshef et al., "Strengthening agricultural decisions in countries at risk of food insecurity: The GEOGLAM crop monitor for early warning," *Remote Sens. Environ.*, vol. 237, 2020, Art. no. 111553. [Online]. Available: <https://linkinghub.elsevier.com/retrieve/pii/S0034425719305735>
- [6] S. Fritz et al., "A comparison of global agricultural monitoring systems and current gaps," *Agricultural Syst.*, vol. 168, pp. 258–272, 2019. [Online]. Available: <https://linkinghub.elsevier.com/retrieve/pii/S0308521X17312027>
- [7] C. Nakalembe et al., "A review of satellite-based global agricultural monitoring systems available for africa," *Glob. Food Secur.*, vol. 29, 2021, Art. no. 100543. [Online]. Available: <https://linkinghub.elsevier.com/retrieve/pii/S2211912421000523>
- [8] I. Becker-Reshef et al., "Monitoring global croplands with coarse resolution earth observations: The global agriculture monitoring (GLAM) project," *Remote Sens.*, vol. 2, no. 6, pp. 1589–1609, 2010 [Online]. Available: <http://www.mdpi.com/2072-4292/2/6/1589>
- [9] S. B. Traore et al., "AGRHYMET: A drought monitoring and capacity building center in the west africa region," *Weather Climate Extremes*, vol. 3, pp. 22–30, 2014. [Online]. Available: <https://linkinghub.elsevier.com/retrieve/pii/S2212094714000279>
- [10] B. Wu, J. Meng, Q. Li, N. Yan, X. Du, and M. Zhang, "Remote sensing-based global crop monitoring: Experiences with China's CropWatch system," *Int. J. Digit. Earth*, vol. 7, no. 2, pp. 113–137, 2014. [Online]. Available: <http://www.tandfonline.com/doi/abs/10.1080/17538947.2013.821185>
- [11] I. Becker-Reshef et al., "The GEOGLAM crop monitor for AMIS: Assessing crop conditions in the context of global markets," *Glob. Food Secur.*, vol. 23, pp. 173–181, 2019. [Online]. Available: <https://linkinghub.elsevier.com/retrieve/pii/S221191241830155X>
- [12] D. Swets, B. Reed, J. Rowland, and S. Marko, "A weighted least-squares approach to temporal NDVI smoothing," *From Image Inf.: 1999 ASPRS (Ame. Soci. Photogrammetry Remote Sens.) Annu. Conf.*, May 17–21, 1999, Portland Oregon.
- [13] A. Pérez-Hoyos, A. Udías, and F. Rembold, "Integrating multiple land cover maps through a multi-criteria analysis to improve agricultural monitoring in Africa," *Int. J. Appl. Earth Observation Geoinformation*, vol. 88, 2020, Art. no. 102064. [Online]. Available: <https://linkinghub.elsevier.com/retrieve/pii/S0303243419309146>
- [14] C. Funk et al., "Recognizing the famine early warning systems network: Over 30 years of drought early warning science advances and partnerships promoting global food security," *Bull. Amer. Meteorological Soc.*, vol. 100, no. 6, pp. 1011–1027, 2019. [Online]. Available: <https://journals.ametsoc.org/view/journals/bams/100/6/bams-d-17-0233.1.xml>
- [15] WFP, "Vulnerability analysis and mapping food security analysis at the world food programme," 2018. [Online]. Available: <https://docs.wfp.org/api/documents/WFP-0000040024/download/>
- [16] P. H. Eilers, V. Pesendorfer, and R. Bonifacio, "Automatic smoothing of remote sensing data," in *Proc. 9th Int. Workshop Anal. Multitemporal Remote Sens. Images*, 2017, pp. 1–3. [Online]. Available: <https://ieeexplore.ieee.org/document/8076705/>
- [17] F. Rembold et al., "ASAP: A new global early warning system to detect anomaly hot spots of agricultural production for food security analysis," *Agricultural Syst.*, vol. 168, pp. 247–257, 2019. [Online]. Available: <https://linkinghub.elsevier.com/retrieve/pii/S0308521X17309095>
- [18] M. Meroni et al., The Warning Classification Scheme of ASAP: Anomaly hot Spots of Agricultural Production, v4.0: Technical Description of Warning Classification System v4.0 (JRC Technical reports). Publications Office, 2019. [Online]. Available: https://mars.jrc.ec.europa.eu/asap/files/asap_warning_classification_v_4_0.pdf
- [19] R. Van Hoolst et al., "FAO's AVHRR-based agricultural stress index system (ASIS) for global drought monitoring," *Int. J. Remote Sens.*, vol. 37, no. 2, pp. 418–439, 2016. [Online]. Available: <http://www.tandfonline.com/doi/full/10.1080/01431161.2015.1126378>
- [20] O. Rojas, "Next generation agricultural stress index system (ASIS) for agricultural drought monitoring," *Remote Sens.*, vol. 13, no. 5, 2021, Art. no. 959. [Online]. Available: <https://www.mdpi.com/about/announcements/784>
- [21] OECD and Sahel and West Africa Club, An Atlas of the Sahara-Sahel: Geography, Economics and Security (West African Studies). OECD, 2014. [Online]. Available: https://www.oecd-ilibrary.org/agriculture-and-food/an-atlas-of-the-sahara-sahel_9789264222359-en
- [22] J. A. Dixon, D. P. Gibbon, and A. Gulliver, "Farming systems and poverty: Improving farmers' livelihoods in a changing world," *Food Agriculture Org. United Nations (FAO) World Bank*, 2001, Art. no. 420.
- [23] S. E. Nicholson, *Climate of the Sahel and West Africa*. London, U.K.: Oxford Univ. Press, 2018. [Online]. Available: <http://climatescience.oxfordre.com/view/10.1093/acrefore/9780190228620.001.0001/acrefore-9780190228620-e-510>
- [24] Aurich, Christopher, Dixon, John, Boffa, Jean-Marc, and Dennis Garrity, "Farming systems of africa," in Atlas of African Agriculture Research and Development. Washington, DC, USA: International Food Policy Research Institute (IFPRI), 2014, pp. 14–15. [Online]. Available: <https://ebrary.ifpri.org/utils/getfile/collection/p15738coll2/id/128741/filename/128952.pdf>

- [25] Z. Nouaceur and O. Murarescu, "Rainfall variability and trend analysis of rainfall in west africa (Senegal, Mauritania, Burkina Faso)," *Water*, vol. 12, no. 6, 2020, Art. no. 1754. [Online]. Available: <https://www.mdpi.com/2073-4441/12/6/1754>
- [26] S. M. Herrmann, M. Brandt, K. Rasmussen, and R. Fensholt, "Accelerating land cover change in west africa over four decades as population pressure increased," *Commun. Earth Environ.*, vol. 1, no. 1, p. 53, 2020. [Online]. Available: <http://www.nature.com/articles/s43247-020-00053-y>
- [27] CILSS, "Landscapes of west africa—A window on a changing world," *Ouagadougou, Burkina Faso, CILSS*, 2016, Art. no. 219. [Online]. Available: <https://eros.usgs.gov/westafrica/sites/default/files/ebook-English/index.html>
- [28] J. Latham, R. Cumani, I. Rosati, and M. Bloise, "FAO global land cover (GLC-SHARE) beta-release database," *FAO, Land Water Division*, p. 40, 2014. [Online]. Available: <https://www.fao.org/uploads/media/glc-share-doc.pdf>
- [29] M. A. White, P. E. Thornton, and S. W. Running, "A continental phenology model for monitoring vegetation responses to interannual climatic variability," *Glob. Biogeochemical Cycles*, vol. 11, no. 2, pp. 217–234, 1997.
- [30] E. Hovmöller, "The trough-and-ridge diagram," *Tellus*, vol. 1, no. 2, pp. 62–66, 1949.
- [31] I. McCallum, M. Obersteiner, S. Nilsson, and A. Shvidenko, "A spatial comparison of four satellite derived 1 km global land cover datasets," *Int. J. Appl. Earth Observation Geoinformation*, vol. 8, no. 4, pp. 246–255, 2006. [Online]. Available: <https://linkinghub.elsevier.com/retrieve/pii/S0303243405001212>
- [32] J. Brown, D. Howard, B. Wylie, A. Frieze, L. Ji, and C. Gacke, "Application-ready expedited MODIS data for operational land surface monitoring of vegetation condition," *Remote Sens.*, vol. 7, no. 12, pp. 16226–16240, 2015. [Online]. Available: <http://www.mdpi.com/2072-4292/7/12/15825>
- [33] S. E. Cotillon, "West Africa land use and land cover time series," *USGS, Reston, VA, Fact Sheet 2017-3004*, 2017. Available: <https://pubs.usgs.gov/fs/2017/3004/fs20173004.pdf>
- [34] A. Mechiche-Alami and A. M. Abdi, "Agricultural productivity in relation to climate and cropland management in west africa," *Sci. Rep.*, vol. 10, no. 1, 2020, Art. no. 3393. [Online]. Available: <http://www.nature.com/articles/s41598-020-59943-y>
- [35] W. Zhang, M. Brandt, X. Tong, Q. Tian, and R. Fensholt, "Impacts of the seasonal distribution of rainfall on vegetation productivity across the sahel," *Biogeosciences*, vol. 15, no. 1, pp. 319–330, 2018. [Online]. Available: <https://bg.copernicus.org/articles/15/319/2018/>
- [36] X. Tong et al., "Revisiting the coupling between NDVI trends and cropland changes in the sahel drylands: A case study in western Niger," *Remote Sens. Environ.*, vol. 191, pp. 286–296, 2017. [Online]. Available: <https://linkinghub.elsevier.com/retrieve/pii/S003442571730041X>
- [37] M. C. Hansen et al., "Humid tropical forest clearing from 2000 to 2005 quantified by using multitemporal and multiresolution remotely sensed data," *Proc. Nat. Acad. Sci.*, vol. 105, no. 27, pp. 9439–9444, 2008.
- [38] P. Potapov et al., "Global maps of cropland extent and change show accelerated cropland expansion in the twenty-first century," *Nature Food*, vol. 3, no. 1, pp. 19–28, 2022.
- [39] E. L. Garrouette, A. J. Hansen, and R. L. Lawrence, "Using NDVI and EVI to map spatiotemporal variation in the biomass and quality of forage for migratory elk in the greater yellowstone ecosystem," *Remote Sens.*, vol. 8, no. 5, p. 404, 2016. [Online]. Available: <https://www.mdpi.com/about/announcements/784>
- [40] L. Ji and A. J. Peters, "Performance evaluation of spectral vegetation indices using a statistical sensitivity function," *Remote Sens. Environ.*, vol. 106, no. 1, pp. 59–65, 2007.
- [41] G. Fischer et al., "Global agro-ecological zones V4—model documentation," Rome, FAO, 2021. [Online]. Available: <https://doi.org/10.4060/cb4744en>
- [42] C. O. Justice and I. Becker-Reshef, "Report from the workshop on developing a strategy for global agricultural monitoring in the framework of group on earth observations (GEO)," UN FAO, Geography Dept., Univ. Maryland, Jul. 2007, p. 66. [Online]. Available: https://www.earthobservations.org/documents/cop_ag_gams/200707_01/20070716_geo_igol_ag_workshop_report.pdf
- [43] L. Leroux, M. Castets, C. Baron, M.-J. Escorihuela, A. Bégué, and D. Lo Seen, "Maize yield estimation in west africa from crop process-induced combinations of multi-domain remote sensing indices," *Eur. J. Agronomy*, vol. 108, pp. 11–26, 2019. [Online]. Available: <https://linkinghub.elsevier.com/retrieve/pii/S116103011830354X>
- [44] H. Deléglise et al., "Linking heterogeneous data for strengthening food security systems—Case of agricultural production in west africa," in *Proc. 4th Int. Conf. Glob. Food Secur.*, 2020. [Online]. Available: https://www.umr-tetis.fr/jdownloads/animations-scientifiques/Poster_GFS2020_Food_Security_News_Mining.pdf



Agnès Bégué received the Ph.D. degree in physics from the University Paris VII, Paris, France, in 1991.

She has initial training in agricultural engineering. After a 2-year Postdoctoral Research Position spent with the University of Maryland, College Park, MD, USA, and another 2-year spent at CNES (France), she got a permanent position in 1995 with CIRAD, a French scientific organization specialized in development-oriented agricultural research for the tropics and subtropics, Montpellier, France. Her research interests include the development of satellite data-based models and methods to assess land productivity and characterize cropping practices, in particular for smallholder agriculture in Africa.



Simon Madec received the Ph.D. degree in agonomic science from the University of Avignon, Avignon, France, in 2019.

He is currently a Computer Vision Engineer. After three years of research on field crop phenotyping with the INRAE research institute, Paris, France. He joined the CIRAD, Montpellier, France, in 2021 after two years of Postdoc with the University of Tokyo, Tokyo, Japan, University of Queensland, Brisbane, QLD, Australia, and Arvalis (France). He has experience in the development of algorithms for image segmentation, object detection, and 3-D point cloud analysis. His research now focuses on the use of machine learning/deep learning and remote sensing for the estimation of agricultural variables, crop practices, in particular for food security.



Louise Lemettais received the double master's degree in geography of risk from the University of Grenoble, Grenoble, France, in 2020, and in science in geomatics in environment and planning from the University of Toulouse, Toulouse, France, in 2021.

She is currently a Geomatics Engineer. She has several research experiences with CIRAD, a French scientific organization specialized in development-oriented agricultural research for the tropics and subtropics, Montpellier, France. She is currently a Research Engineer with IRD, Marseille, France, a French scientific organization that addresses international development issues with its partners in the South. Her research work focuses on the development of satellite-based methods to assess vegetation dynamics in relation to climate change and agriculture.



Louise Leroux is currently a Researcher with CIRAD institute, AiDA, Montpellier, France, unit, which works on agroecology and sustainable intensification of annual crops production in terms of quantity and also quality where its relevant, in a particularly constrained tropical environment. She is currently a Geographer with a strong background in remote sensing applied to agricultural monitoring. She focuses her research on the use of remote sensing technologies combined with statistical or biophysical modeling to improve the cropping systems descriptions (where

are the crop areas and what kind of crops, what are the agricultural practices, what are the interactions with the surrounding landscape? etc.) and improve the assessment of agronomical and environmental performances of smallholder cropping systems. Over the last years she worked mainly in West Africa, with a focus on agroforestry systems. She was previously seconded to Centre de Suivi Ecologique, Dakar, Senegal, and she is currently with the IITA Nairobi, Nairobi, Kenya, where she conducts her research mainly in Ethiopia and Rwanda.



Roberto Interdonato received the Ph.D. degree in computer engineering from the University of Calabria, Arcavacata, Italy, in 2015. His Ph.D. dissertation was titled “novel ranking problems in information networks.”

He is currently a Research Scientist with CIRAD, UMR TETIS, Montpellier, France. He was previously a Postdoctoral Researcher with the University of La Rochelle, La Rochelle, France, Uppsala University, Uppsala, Sweden, and University of Calabria, Arcavacata, Italy. His research interests include the design of data science techniques applied to the analysis of complex networks (e.g., social media networks, trust networks, semantic networks, bibliographic networks) and the extraction of information from remote sensing data. His most recent contributions concern the implementation of deep learning methods for land use classification based on the analysis of time series of multisensor satellite images (optical, radar, high/very high spatial resolution), the application of complex network analysis techniques for the extraction of spatialized indicators (landscape, socio-economic) from multisource data (remote sensing, survey data, statistics, social networks, etc.). His thematic interests mainly concern the characterization of tropical agricultural landscapes, the production of spatial information for food security and the analysis of the transnational land trade market. On these topics, he has coauthored journal articles and conference papers, organized workshops, presented tutorials at international conferences and developed practical software tools.

MD, USA, and an Adjunct Professor with the University of Strasbourg, Strasbourg, France. Her work is focused on the application of satellite observations for agricultural monitoring from the field to global scales, supporting decisions in food security, sustainability, and agricultural markets. She worked closely with national and international partners to initiate the GEO Global Agricultural Monitoring (GEOGLAM) Program, adopted by the G20 in 2011 under the action plan on food price volatility and agriculture where she leads the Crop Monitor initiative.



Inbal Becker-Reshef received the Ph.D. degree in geographical sciences from the University of Maryland, College Park, MD, USA, in 2012.

She is currently the Director of NASA Harvest which is NASA's Global Program on Food Security and Agriculture, made up of a diverse consortium of over 50 partners from the public and private sectors, focused on advancing the use of satellite observations across the agricultural sector. She is currently a Research Professor with the Department of Geographical Sciences, University of Maryland, College Park,

MD, USA, and an Adjunct Professor with the University of Strasbourg, Strasbourg, France. Her work is focused on the application of satellite observations for agricultural monitoring from the field to global scales, supporting decisions in food security, sustainability, and agricultural markets. She worked closely with national and international partners to initiate the GEO Global Agricultural Monitoring (GEOGLAM) Program, adopted by the G20 in 2011 under the action plan on food price volatility and agriculture where she leads the Crop Monitor initiative.



Christina Justice received the M.S. degree in geographical sciences from the University of Maryland, College Park, MD, USA, in 2015.

She is currently a Remote Sensing Researcher with the Geographical Sciences Department, University of Maryland, the NASA Harvest Food Security and Early Warning Co-Lead and Lead of the GEOGLAM Crop Monitor for Early Warning. Her research interests are in the use of EO for agricultural monitoring over smallholder cropping systems and bridging the gap between agricultural land use practices and remotely sensed information to better inform agriculture policies and decision making in support of food security.

MD, USA, and an Adjunct Professor with the University of Strasbourg, Strasbourg, France. Her work is focused on the application of satellite observations for agricultural monitoring from the field to global scales, supporting decisions in food security, sustainability, and agricultural markets. She worked closely with national and international partners to initiate the GEO Global Agricultural Monitoring (GEOGLAM) Program, adopted by the G20 in 2011 under the action plan on food price volatility and agriculture where she leads the Crop Monitor initiative.



Brian Barker received the masters of arts in geographic science from the University of Maryland, College Park, MD, USA, in 2012.

He is currently the co-lead of NASA Harvest's working area on crop conditions. As part of the work, he leads the GEOGLAM Crop Monitor for AMIS (CM4AMIS), which is a monthly crop monitoring report active since 2013, covering the main food crops (wheat, maize, rice, and soybeans) in the major producing and exporting countries of the world, within the FAO Agricultural Market Information System

(AMIS) Market Monitor and as a stand-alone publication. Expanding on the work of the CM4AMIS, he is currently leading the GEOGLAM Global Crop Monitor in partnership with the International Grains Council (IGC), which provides a complete global overview of crop conditions. He is currently a member of the Expert Group on Early-warning system for the Mediterranean region (EWS-Med) for the Mediterranean Agricultural Markets Information Network (MED-AMIN) initiative.



Hervé Kerdilès received the obtained agricultural engineer degree and the Ph.D. degree in mathematics and computer sciences from the Institut National Agronomique Paris-Grignon, Paris, France, in 1988 and 1995, respectively.

He is currently an Agricultural Engineer. He has been with the Monitoring Agricultural Resources (MARS) unit, now Food Security unit of Directorate D “Sustainable Resources”—with the Joint Research Centre of the European Commission, Ispra, Italy, since 2000. His research focuses on crop monitoring

and early warning based on low resolution imagery and meteo data; crop yield estimation based on yield time series and (remote sensing or meteo) indicators; crop area estimation based on remote sensing and ground survey, mainly on food insecure countries (Africa, but also middle-east; central, south, and south-east Asia, DPRK).



Michele Meroni received the University degree in environmental sciences from the University of Milan, Milan, Italy, and the Ph.D. degree in forest ecology from the University of Tuscia, Viterbo, Italy, in 1998 and 2005, respectively.

He has been working with different sources of remote sensing data, from field spectroscopy to airborne hyperspectral and satellite multispectral and multitemporal imagery. He is currently working for the Food Security Unit of the Joint Research Centre, European Commission, Ispra, Italy, using remote

sensing and meteorological data to characterize the state and evolution of agricultural and pastoral areas in Africa.